J. Iron Steel Res. Int.
https://doi.org/10.1007/s42243-024-01245-y

ORIGINAL PAPER

Mechanism of thermal compressive strength evolution of carbon-bearing iron ore pellet without binders during reduction process

Hong-tao Wang[1] · Yi-bin Wang[1] · Shi-xin Zhu[1] · Qing-min Meng[1] · Tie-jun Chun[1] · Hong-ming Long[1,2]

Received: 19 February 2024 / Revised: 21 March 2024 / Accepted: 26 March 2024

Abstract
Against the background of "carbon peak and carbon neutrality," it is of great practical significance to develop non-blast furnace ironmaking technology for the sustainable development of steel industry. Carbon-bearing iron ore pellet is an innovative burden of direct reduction ironmaking due to its excellent self-reducing property, and the thermal strength of pellet is a crucial metallurgical property that affects its wide application. The carbon-bearing iron ore pellet without binders (CIPWB) was prepared using iron concentrate and anthracite, and the effects of reducing agent addition amount, size of pellet, reduction temperature and time on the thermal compressive strength of CIPWB during the reduction process were studied. Simultaneously, the mechanism of the thermal strength evolution of CIPWB was revealed. The results showed that during the low-temperature reduction process (300–500 °C), the thermal compressive strength of CIPWB linearly increases with increasing the size of pellet, while it gradually decreases with increasing the anthracite ratio. When the CIPWB with 8% anthracite is reduced at 300 °C for 60 min, the thermal strength of pellet is enhanced from 13.24 to 31.88 N as the size of pellet increases from 8.04 to 12.78 mm. Meanwhile, as the temperature is 500 °C, with increasing the anthracite ratio from 2% to 8%, the thermal compressive strength of pellet under reduction for 60 min remarkably decreases from 41.47 to 8.94 N. Furthermore, in the high-temperature reduction process (600–1150 °C), the thermal compressive strength of CIPWB firstly increases and then reduces with increasing the temperature, while it as well as the temperature corresponding to the maximum strength decreases with increasing the anthracite ratio. With adding 18% anthracite, the thermal compressive strength of pellet reaches the maximum value at 800 °C, namely 35.00 N, and obtains the minimum value at 1050 °C, namely 8.60 N. The thermal compressive strength of CIPWB significantly depends on the temperature, reducing agent dosage, and pellet size.

Keywords Non-blast furnace ironmaking · Carbon-bearing iron ore pellet · Reduction reaction · Thermal compressive strength · Mechanism

1 Introduction

Steel industry is one of the significant pillar industries to ensure national security and drive economic and social development. According to the National Bureau of Statistics of China, the Chinese crude steel and blast furnace pig iron production in 2023 reached approximately 1.019 billion tons and 871 million tons, accounting for 53.97% of global crude steel production and 67.70% of global pig iron production, respectively. The blast furnace–basic oxygen furnace process, also known as the long process, is the most prevalent method for steel production because it is highly efficient and operated on a large scale [1–5]. With the gradual implementation of "carbon peak and carbon neutrality," "ultra-low emission" in China, low carbon, green, and high efficiency have become the development direction of steel industry [6–8], leading to serious challenges for the long process. Although blast furnace has distinct advantages as an ironmaking reactor, it also has some shortcomings, such as a lengthy production

✉ Qing-min Meng
mengqingmin@ahut.edu.cn

✉ Hong-ming Long
yaflhm@126.com

[1] School of Metallurgical Engineering, Anhui University of Technology, Ma'anshan 243032, Anhui, China

[2] Key Laboratory of Metallurgical Emission Reduction and Resource Recycling (Ministry of Education), Anhui University of Technology, Ma'anshan 243002, Anhui, China

Published online: 27 May 2024

process, a large investment scale, high energy consumption, serious environmental pollution (especially the coking and sintering process), and heavy reliance on superior coking coal resources [9–11]. Non-blast furnace ironmaking technology does not rely on the coke and sinter, but it has a limited monomer production capacity [12–15]. Thus, the development of non-blast furnace ironmaking technology is of great practical significance for the sustainable and green development of steel industry.

Nowadays, the non-blast furnace ironmaking process primarily consists of direction reduction and smelting reduction. Carbon-bearing iron ore pellet (CIP) is considered to be an innovative burden for the direct reduction ironmaking due to its excellent self-reducing property [16–21], and the thermal strength of CIP is a crucial metallurgical property that significantly affects its wide application in low-carbon iromaking [22–28]. Compared with oxidized pellet, CIP contains a certain amount of solid reducing agents, which can contribute to the lower shatter strength and drying strength of green pellet. Simultaneously, the physical structure of CIP is deteriorated during the reduction process due to the gasification reaction of carbon, reduction of iron oxides, and thermal stress, making it difficult for CIP to meet the production requirements of high-efficiency reactors in terms of thermal strength. Currently, the CIP has only been successfully applied in the rotary hearth furnace (RHF) [29], primarily due to the low strength requirement of pellets resulting from the thin material layer and low pellet load during the reduction process. However, the RHF also suffers from issues such as high energy consumption and low production efficiency. Therefore, improving the thermal strength of CIP during the reduction process is crucial for realizing multiple burden layers of RHF [30]. Yang et al. [30, 31] prepared cold-pressed carbon-bearing pellet using iron and carbon-containing solid waste and composite binder, and studied the effects of reduction conditions on the strength of green pellet and the post-reduction strength of pellet. The results indicated that the post-reduction strength of pellet can be improved by appropriately increasing the reduction temperature and time. Moreover, the effects of binders such as bentonite, sodium silicate, and hydroxypropyl methylcellulose (HPMC) on the shatter strength and compressive strength of cold-pressed carbon-containing pellet were investigated by Lu et al. [32]. It was found that adding HPMC can evidently improve the strength of pellet. Furthermore, Zhang et al. [33] prepared the carbon-containing pellet utilizing iron ore, bituminous coal, bentonite, and organic binder (HC), and investigated the effect of the binder dosage on the pellet strength. With increasing the dosage of HC and bentonite, the compressive strength of green pellet is enhanced. Simultaneously, the shatter strength of green pellet is improved with increasing the amount of HC, while there is no significant variation on the shatter strength with increasing the bentonite consumption. Meanwhile, the cylindrical carbon-bearing pellet was prepared by Wu et al. [34] with using electric furnace dust, anthracite and bentonite, and the effects of water content, amount of bentonite, pressure, and C/O (the molar ratio of fixed carbon in coal to oxygen in iron oxide) on the pellet strength were studied. The results presented that the shatter strength of green pellet is more affected by the above factors compared to the compressive strength, and the effect of water content and bentonite ratio is more significant. In addition, Zhang et al. [35] investigated the compressive strength of carbon-bearing pellet with MgO, and found that with adding 6% coal and 1.5% bentonite, the compressive strength of pellet firstly increases and then decreases with increasing the temperature, and the optimized temperature for the maximum compressive strength of pellet is 1250–1300 °C. Most of the aforementioned studies focused on the effects of process parameters and reduction conditions on the cold strength or post-reduction strength of pellet under the action of binders, but there are few studies involving the particle interaction of iron-containing raw materials and solid reducing agents, as well as their influence on the thermal strength of pellet during the reduction process.

In this work, the carbon-bearing iron ore pellet without binders (CIPWB) was prepared by disk pelletizer using iron ore concentrate and anthracite as raw materials. Furthermore, the effects of anthracite addition ratio, reduction temperature and time on the thermal compressive strength of CIPWB during the reduction process were experimentally investigated. Meanwhile, the evolution law of microstructure and phase composition of CIPWB was elucidated through modern analysis and testing technology. This work could provide a theoretical basis and data support for promoting the incremental application of carbon-bearing pellet and the development of non-blast furnace ironmaking technology.

2 Experimental

2.1 Raw materials

The raw materials used in this work mainly include iron ore concentrate and anthracite. The chemical composition of iron ore concentrate is listed in Table 1. It can be seen that the total iron (TFe) content is approximately 61.40 wt.% and the FeO content is about 23.50 wt.%, indicating that the iron ore belongs to magnetite concentrate. The proximate analysis of anthracite is presented in Table 2. Clearly, the fixed carbon content and the ash content of anthracite are 78.77 and 13.29 wt.%, respectively. Meanwhile, the

Table 1 Chemical composition of iron ore concentrate (wt.%)

TFe	FeO	SiO_2	Al_2O_3	CaO	MgO	P	S
61.40	23.50	3.30	1.10	1.00	0.20	0.03	0.33

Table 2 Proximate analysis of anthracite (wt.%)

Fixed carbon	Ash (13.29)					Volatile matter	S_t
	SiO_2	Al_2O_3	CaO	MgO	Fe_2O_3		
78.77	52.81	31.63	1.56	0.86	5.11	6.37	0.58

Fixed carbon, ash, and volatile matter were measured in air dried basis; total sulfur content (S_t) is measured in dried basis

Table 3 Characteristic parameters of size distribution of iron ore concentrate and anthracite powder (μm)

Raw material	*D*10	*D*50	*D*90	*D*(4,3)
Iron ore concentrate	4.73	21.17	48.77	24.32
Anthracite powder	3.97	17.46	44.27	21.39

*D*10—Particle size when cumulative distribution proportion reaches 10%; *D*50—particle size when cumulative distribution proportion is 50%, namely, median size; *D*90—particle size when cumulative distribution proportion reaches 90%

contents of SiO_2 and Al_2O_3 in the ash of coal are relatively high, which are 52.81 and 31.63 wt.%, respectively.

The raw materials were dried at 120 °C for 24 h in a forced-air drying cabinet, followed by ball milling of the iron ore and anthracite. The size distribution characteristics of the raw materials after crushing are presented in Table 3. It can be clearly seen that both iron ore concentrate and anthracite powder exhibit a wide range of particle sizes, with the iron ore concentrate having slightly coarser particles compared to anthracite powder based on the volume average particle size *D*(4,3) [36]. Moreover, Fig. 1 depicts the micromorphologies of iron ore concentrate and anthracite powder. In terms of iron ore concentrate particles, the surface of the large iron ore particle is embedded by some fine particles. However, the particle of anthracite powder is relatively regular, with a round and smooth surface.

2.2 Experimental scheme and procedure

2.2.1 Preparation process of carbon-bearing iron ore pellet without binders

The experimental scheme for preparing the CIPWB under laboratory conditions is presented in Table 4. Initially, the iron ore concentrate and anthracite powder were subjected to a drying process at 120 °C for 24 h. Then, specific amounts of iron ore concentrate and anthracite powder were weighed according to the mass ratio listed in Table 4 and thoroughly mixed to form homogeneous mixture with a total mass of 3 kg for each test. Afterward, 3.0% water (extra adding) was added to the mixtures for pre-wetting treatment, and the treatment time is 2 h. Subsequently, the mixture was pelletized into green pellet using a balling disk pelletizer with a diameter of 1000 mm, and the final moisture of green pellet was controlled at 9.0%. Finally, the green pellets were dried in an oven at 105 °C for 24 h to obtain CIPWB with a diameter of 7–15 mm.

2.2.2 Reduction process of CIPWB and thermal compressive strength testing

The reduction and thermal compressive strength testing of CIPWB were carried out utilizing a thermal strength online testing device, as seen in Fig. 2 [37]. The device comprises four units, namely heating and temperature control, thermal strength measurement, atmosphere regulation, and data acquisition. Firstly, the dried CIPWB was placed into the sample table equipped with an automatic lifting and rotating function in the flat-temperature zone. Subsequently, the pellet was heated to the predetermined temperature with a heating rate of 8 °C/min under argon atmosphere with a flow rate of 5 L/min. Afterward, as the reaction was conducted at a certain time (15–60 min), the thermal compressive strength of pellet was tested and automatically recorded by the data acquisition system. For each test, ten pellets were measured, and the average value was used as the final experimental result.

2.3 Characterization methods

The X-ray diffraction (XRD) patterns of CIPWB were analyzed using an X-ray diffractometer (MPDDY2094, PANalytical B.V. Corporation, the Netherlands). Cu Kα radiation (40 kV, 40 mA, wavelength 0.154 nm) was employed as the X-ray source, and the scanning range varied from 5° to 90°. The microstructure of reduced

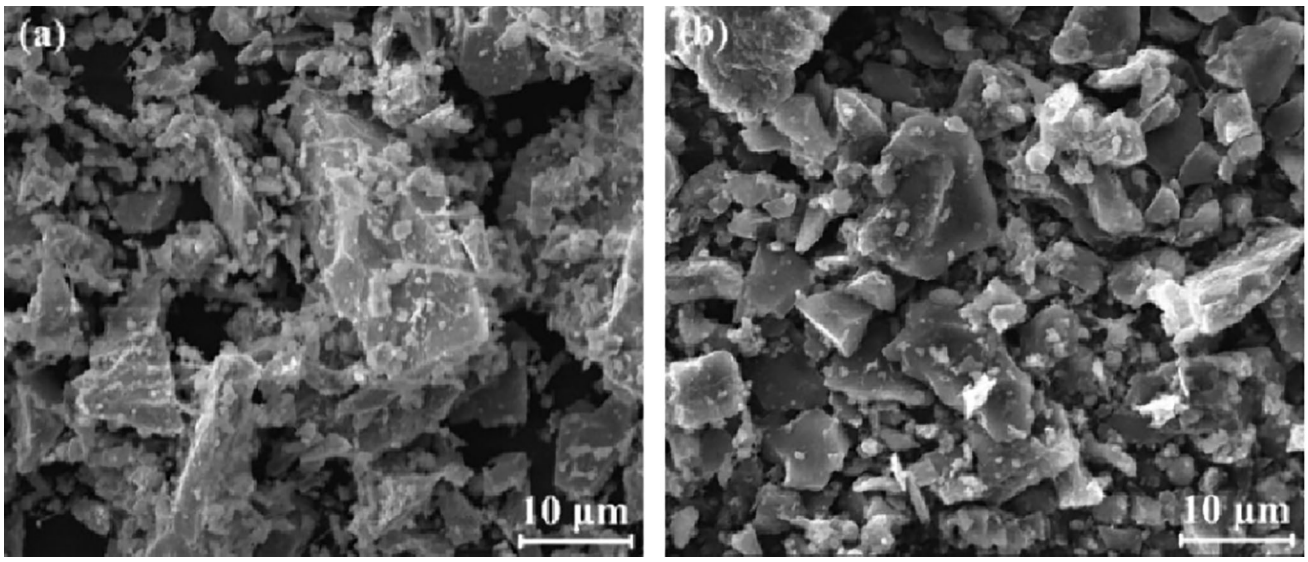

Fig. 1 Microtopography of iron ore concentrate (**a**) and anthracite powder (**b**)

Table 4 Experimental scheme for preparation of CIPWB under laboratory conditions

No.	Addition ratio of anthracite/%	Addition ratio of iron ore/%	Moisture/%	C/O
1	2	98	9.0	0.1
2	4	96	9.0	0.2
3	6	94	9.0	0.3
4	8	92	9.0	0.4
5	18	82	9.0	1.0

CIPWB was examined using a scanning electron microscope (SEM) equipped with an energy dispersive X-ray spectrometer (EDS, Ultra Plus, Zeiss, Germany).

3 Results and discussion

3.1 Thermal compressive strength of CIPWB during low-temperature reduction process

3.1.1 Effect of pellet size on thermal compressive strength of CIPWB

Considering the stepwise reduction of iron oxide, the reduction process of CIPWB in this work is divided into two stages, namely, low-temperature reduction stage (300–500 °C) and high-temperature reduction stage (600–1050 °C). Figure 3 shows the effects of pellet size on the thermal compressive strength of CIPWB when the reduction temperature is 300 °C. It can be clearly seen that increasing the size of pellet gradually enhances the thermal compressive strength of CIPWB during low-temperature reduction. As the reduction temperature is approximately 300 °C and the reduction time is 30 min, the thermal compressive strength of CIPWB with adding 2% anthracite is enhanced from 9.73 to 31.03 N with increasing the size of pellet from 8.14 to 13.62 mm. Furthermore, when the CIPWB with 8% anthracite is reduced at 300 °C for 60 min, increasing the pellet size from 8.04 to 12.78 mm heightens the thermal compressive strength from 13.24 to 31.88 N. Meanwhile, the effects of pellet size on the thermal compressive strength of CIPWB as the reduction temperature is 500 °C are illustrated in Fig. 4. Clearly, under 30 min reduction for 30 min, the thermal compressive strength of CIPWB with adding 2% anthracite increases from 50.78 to 69.12 N with increasing the pellet size from 7.84 to 13.46 mm. Similarly, when the anthracite ratio is 8%, increasing the pellet size from 7.78 to 13.10 mm reinforces the thermal compressive strength of CIPWB under reduction for 60 min from 6.73 to 12.31 N.

3.1.2 Effect of anthracite addition ratio on thermal compressive strength of CIPWB

The results depicted in Figs. 3 and 4 clearly demonstrate that during the low-temperature reduction process, the thermal compressive strength of CIPWB basically increases linearly with increasing the size of pellet. To further elucidate the influence of anthracite addition ratio on the thermal compressive strength of pellet, the averaging treatment was taken for both pellet size and corresponding thermal strength values shown in Figs. 3 and 4. The data averaging process is conducted as follows: firstly, the pellet sizes of tested samples at identical reduction temperature

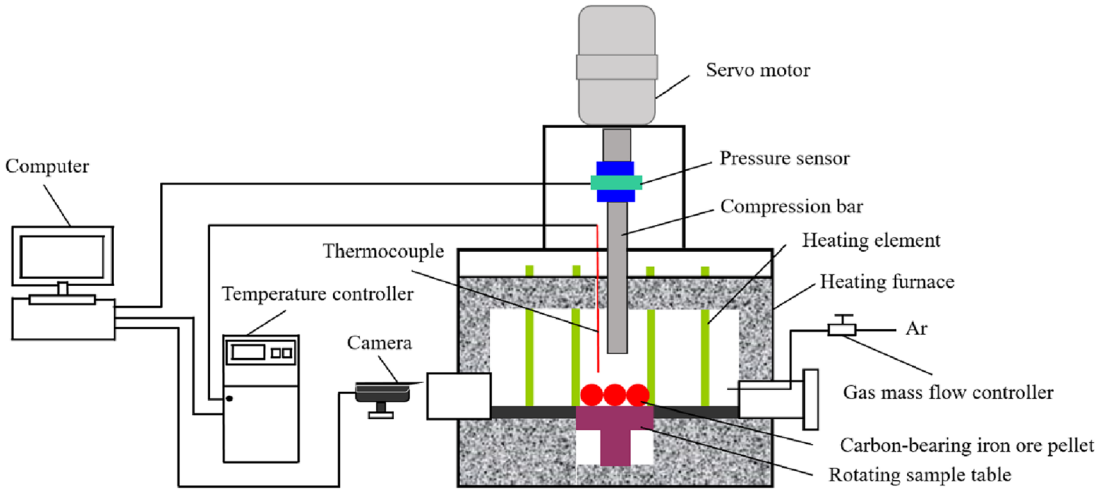

Fig. 2 Schematic diagram of thermal compressive strength testing device for CIPWB

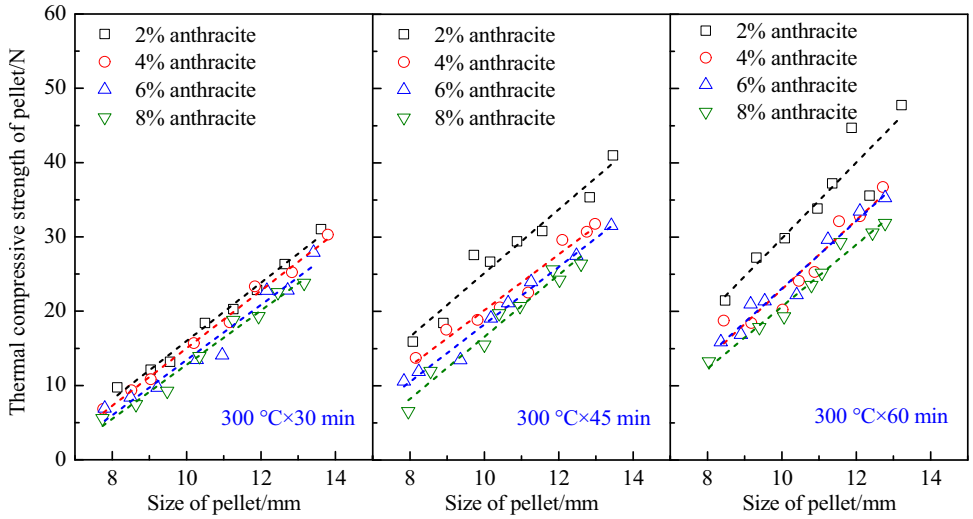

Fig. 3 Effect of pellet size on thermal compressive strength of CIPWB during reduction process at 300 °C

and time were averaged; subsequently, and the corresponding thermal compressive strengths were also averaged. The results of the averaging treatment demonstrate that the average values of pellet size under different conditions in Figs. 3 and 4 are all concentrated in the range of 10.50–11.00 mm, indicating that the averaging treatment can basically mitigate the influence of pellet size. Afterward, the addition ratio of anthracite is used as the independent variable, and the averaged value of the thermal compressive strength is applied as the dependent variable, which is given in Fig. 5. It can be obviously found that when the temperature is approximately 300 °C, with increasing the addition ratio of anthracite from 2% to 8%, the thermal compressive strength of CIPWB decreases from 19.24 to 15.07 N after reduction for 30 min and from 34.70 to 23.85 N after reduction for 60 min, and the decreased degrees are approximately 21.67% and 28.01%, respectively. As the temperature is 500 °C, with increasing the addition ratio of anthracite from 2% to 8%, the thermal compressive strength of CIPWB is significantly reduced from 59.70 to 17.17 N under reduction for 30 min and from 41.47 to 8.94 N under reduction for 60 min, and the corresponding decreased degrees are 71.24% and 78.44%, respectively. Also, it can be visibly observed that with increasing the reduction time, the thermal compressive strength of pellet reduced at 300 °C is gradually enhanced. However, the thermal compressive strength of pellet reduced at 500 °C initially increases and then decreases, reaching the maximum value at 45 min. Consequently, the effects of the temperature on the thermal compressive strength of CIPWB are significant and complicated.

The strength of pellet is the macroscopic manifestation of the comprehensive effects resulting from various forces between the raw material particles, including electrostatic

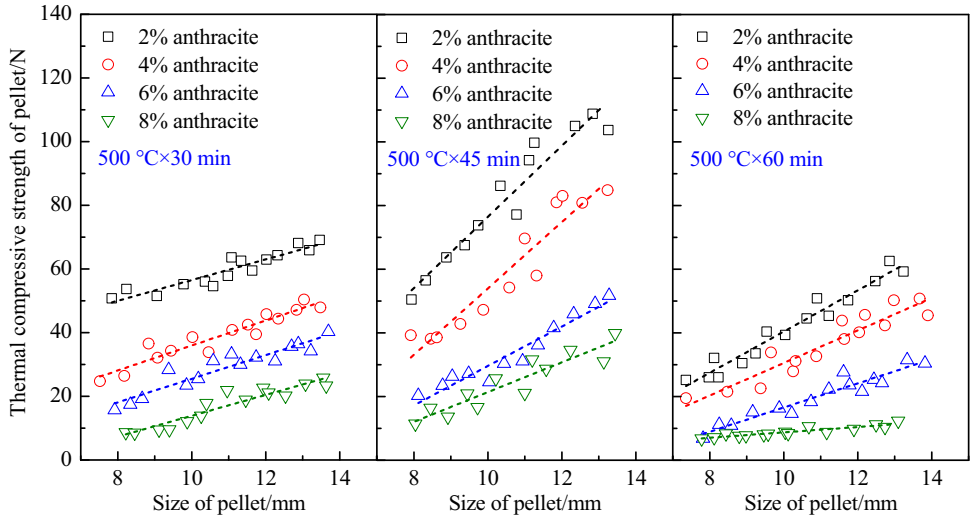

Fig. 4 Effect of pellet size on thermal compressive strength of CIPWB during reduction process at 500 °C

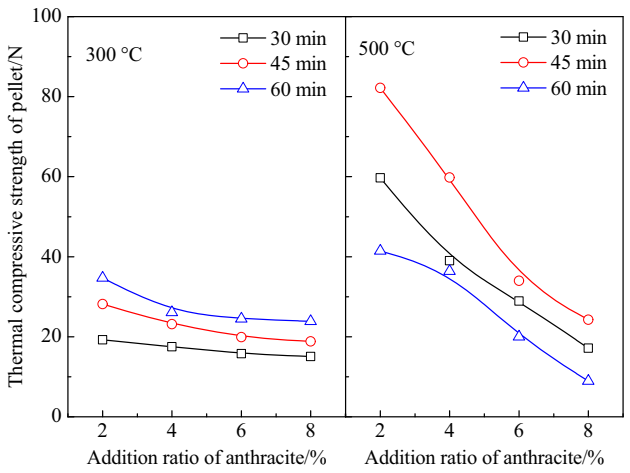

Fig. 5 Effect of anthracite ratio on thermal compressive strength of CIPWB in low-temperature reduction process

force (F_{ele}), van der Waals force (F_{van}), capillary force (F_{cap}), chemical bond force (F_{chem}), meshing force (F_{mes}), and gravity (F_{gra}) [38]. In the case of CIPWB, both capillary force and meshing force play a more dominant role in determining the strength of green pellet compared to other forces. After drying, the primary force responsible for maintaining pellet strength is the meshing force. In consequence, irregularly shaped iron ore particles inside the pellet (as seen in Fig. 1) are more conducive to the meshing between the particles, thereby enhancing the pellet strength. Furthermore, the thermal stress and phase transition of iron oxides during the reduction process of CIPWB also affect the particle meshing. Figure 6 illustrates the microstructure of CIPWB after the reduction under various conditions. During the low-temperature reduction process, magnetite (Fe_3O_4) and hematite (Fe_2O_3) continue to dominate as the iron-bearing phases of CIPWB. However, it is worth noting that there is an observed irregular fragmentation of iron ore particles, with the fragmentation degree being influenced by factors such as the addition amount of anthracite, reduction temperature and time. As observed in Fig. 6a, b, when the temperature is 300 °C, increasing the reduction time from 30 to 60 min leads to the evident fragmentation of iron ore particles within the CIPWB containing 4% anthracite, and the formed fine particles occupied apart of the original space among the particles. The fragmentation can increase the contact area and the meshing degree between the iron ore particles, which is beneficial to improving the thermal strength. The results depicted in Fig. 6b, c also demonstrate that increasing the addition ratio of anthracite from 4% to 8% leads to a deceleration in the fragmentation degree of iron ore particles within the pellet. Meanwhile, it is distinct from Fig. 6b, e that as the anthracite ratio is 4% and the reduction time is 60 min, the fragmentation degree of pellet reduced at 500 °C is higher compared to that at 300 °C. However, the lower anthracite ratio limits the reduction of Fe_2O_3, and thus, the thermal compressive strength of pellet still increases with increasing the reduction temperature from 300 to 500 °C, as seen in Fig. 5. Moreover, when the anthracite ratio is 8% and the reduction time is 60 min, although the fragmentation of iron ore particle can strengthen the interparticle meshing degree, increasing the anthracite amount can promote the reduction of iron oxides. As a result, the expansion caused by the crystal type transformation of iron oxides during the reduction process alters the spatial structure of the particles in the pellet, and the effect of expansion exceeds the fragmentation, as seen in Fig. 6c, f. In consequence, the thermal strength of pellet at 500 °C is lower than that at 300 °C, as seen in Fig. 5. Additionally, when the reduction

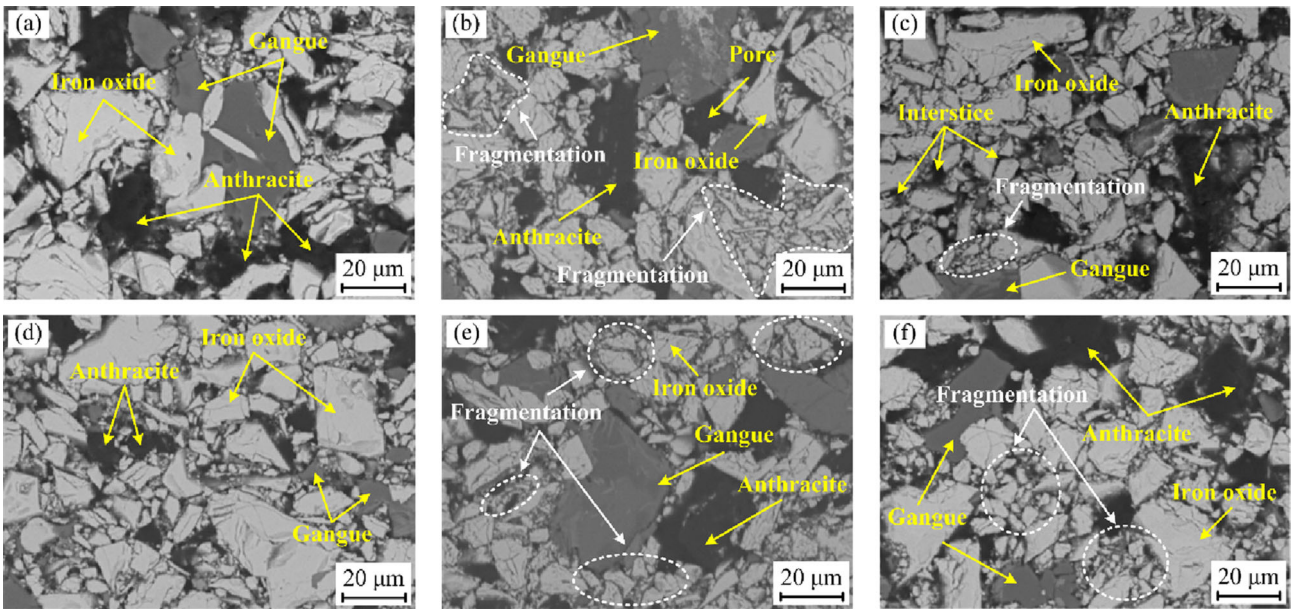

Fig. 6 Microstructure of reduced pellet with adding different ratios of anthracite at low temperature. **a** 4% anthracite at 300 °C and 30 min; **b** 4% anthracite at 300 °C and 60 min; **c** 8% anthracite at 300 °C and 60 min; **d** 4% anthracite at 500 °C and 30 min; **e** 4% anthracite at 500 °C and 60 min; **f** 8% anthracite at 500 °C and 60 min

temperature is 500 °C, with increasing the reduction time from 30 to 60 min, the fragmentation degree of iron ore particles within the CIPWB is augmented. Simultaneously, due to the elevated temperature, there is also an increase in the amount of iron oxide reduced with longer reduction time. As the reduction time increases from 30 to 45 min, the effects on thermal strength are primarily driven by the fragmentation degree rather than the reduction amount, resulting in an overall increase of thermal strength. Furthermore, when the time is prolonged from 45 to 60 min, the effects of the reduction amount surpass the fragmentation degree, which lead to the decrease in the thermal strength.

3.2 Thermal compressive strength of CIPWB during high-temperature reduction process

The thermal compressive strength of CIPWB with the size of 12.5 mm during the high-temperature reduction process (600–1150 °C) under different conditions is presented in Fig. 7. It can be distinctly seen that both temperature and anthracite addition ratio have significant effects on the thermal compressive strength of CIPWB during the high-temperature reduction process. When the anthracite ratio is no more than 8%, the thermal compressive strength of CIPWB firstly increases and then decreases with increasing the reduction temperature, and the temperature corresponding to the maximum thermal strength is concentrated in the range of 1000–1100 °C. As the addition ratio of anthracite is 2%, the thermal compressive strength of

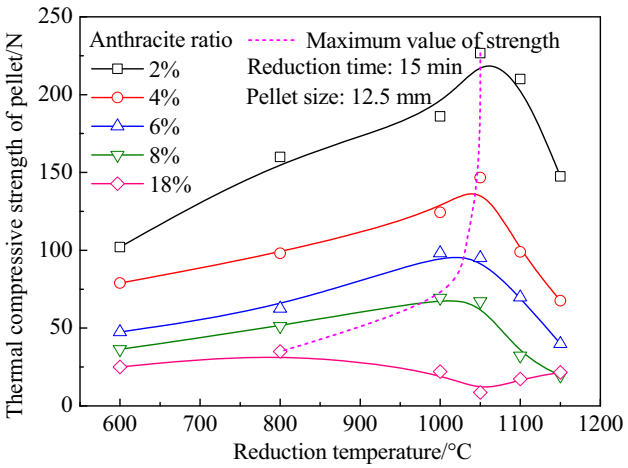

Fig. 7 Effect of temperature on thermal compressive strength of CIPWB during high-temperature reduction process

CIPWB is enhanced from 102.00 to 226.70 N with increasing the reduction temperature from 600 to 1050 °C, while it is reduced to 147.50 N with further increasing the temperature to 1150 °C. Simultaneously, for the CIPWB with adding 8% anthracite, with increasing the reduction temperature from 600 to 1020 °C, the thermal compressive strength of pellet rises from 36.40 to 69.40 N, while it is mitigated to 19.50 N with further increasing the temperature to 1150 °C. In addition, when the ratio of anthracite is 18% (C/O = 1.0), with increasing the temperature, the thermal compressive strength of CIPWB reaches the maximum value at 800 °C (35.00 N), then declines to the minimum value at 1050 °C (only 8.60 N), and

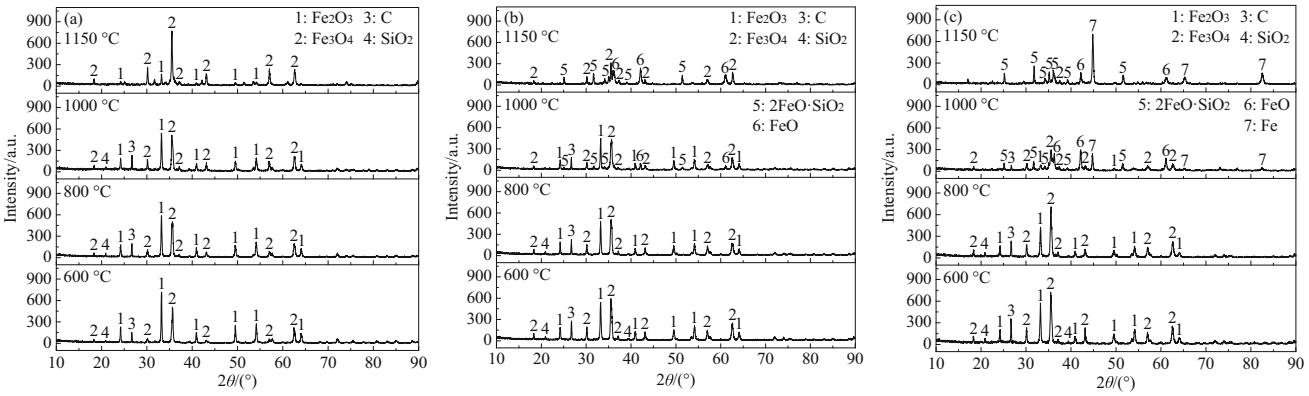

Fig. 8 Phase composition of reduced CIPWB with adding different ratios of anthracite under different temperatures. **a** 4% anthracite; **b** 8% anthracite; **c** 18% anthracite. 2θ—Diffraction angle

subsequently slowly increases. Therefore, with increasing the anthracite ratio, the temperature corresponding to the maximum thermal strength gradually decreases.

When the temperature exceeds 600 °C, the reduction of iron oxide and the gasification reaction of carbon become increasingly evident within the CIPWB. Therefore, both temperature and anthracite ratio can affect the reaction process, internal microstructure, and phase composition of pellet. Figure 8 illustrates the phase composition of reduced CIPWB under different temperatures and anthracite ratios. When the temperature is 600 and 800 °C, the iron-bearing phases within the reduced pellet containing 4%, 8%, and 18% anthracite are predominantly in the form of Fe_2O_3 and Fe_3O_4, and the intensity of Fe_3O_4 peak is strengthened with increasing the temperature and the anthracite ratio. Simultaneously, a small amount of carbon remains within the reduced pellet, which gradually decreases with the temperature rising. When the temperature reaches 1000 °C, the phase composition of pellet with adding 4% anthracite is not much different from that at 800 °C, but the amount of Fe_3O_4 slightly increases. Furthermore, the fayalite ($2FeO{\cdot}SiO_2$) and wustite (FeO) are also observed inside the pellet with adding 8% and 18% anthracite, and the amount of two substances inside the pellet with adding 18% anthracite is significantly more than that inside the pellet with adding 8% anthracite. Moreover, some metallic iron appears inside the pellet containing 18% anthracite. When the temperature is further increased to 1150 °C, the iron-bearing phase of the reduced pellet containing 4% anthracite is predominantly composed of Fe_3O_4. In contrast, with adding 8% anthracite, fayalite and wustite become the main constituents of the iron-bearing phase, accompanied by a small amount of Fe_3O_4. Meanwhile, in the case of a reduced pellet containing 18% anthracite, metallic iron becomes the dominant component in its iron-bearing phase, and a small amount of fayalite and wustite are also observed. At this time, the internal structure of the pellet is mainly consolidated by the metal bond facilitated by the metallic iron crystal.

The microstructure of CIPWB after the reduction under different reduction temperatures and anthracite addition ratios is depicted in Fig. 9. It can be observed from Fig. 9a, b, e, f, i, j that when the reduction temperature is lower than 800 °C, the microstructure of reduced pellet is gradually dense with increasing the temperature, leading to a slight increase in the thermal strength. However, increasing the anthracite ratio gradually leads to a looser microstructure of the reduced pellet, resulting in a decline in its thermal strength. Furthermore, it is also seen from Fig. 9c, g, k that when the reduction temperature is elevated to 1000 °C, the pellet containing 4% and 8% anthracite still retain their intact shape after the reduction, but the edges of the pellet containing 18% anthracite appear blurred, indicating that the reduction reaction significantly occurs upon increasing the anthracite ratio at this temperature. Moreover, as can be seen from Fig. 9d, h, when the reduction temperature is 1150 °C, the iron-containing phase inside the reduced pellet with adding 4% and 8% anthracite is dominated by Fe_3O_4, and the spherical wustite and fayalite are also observed within the latter. Meanwhile, the main iron-bearing phase of the reduced pellet with 18% anthracite is metallic iron, as seen in Fig. 9l, and the metallic iron has been connected, which can improve the thermal strength of the pellet.

Additionally, Fig. 10 shows the porosity and volume shrinkage ratio of CIPWB with adding 18% anthracite during the reduction process. It can be observed that with increasing the temperature, the porosity of reduced pellet firstly increases and then decreases, and the volume shrinkage ratio gradually increases. When the temperature is below 800 °C, there is no significant change in the porosity and shrinkage ratio of the reduced pellet with increasing the temperature. However, as the temperature continues to rise, the reduction reaction of iron oxide and

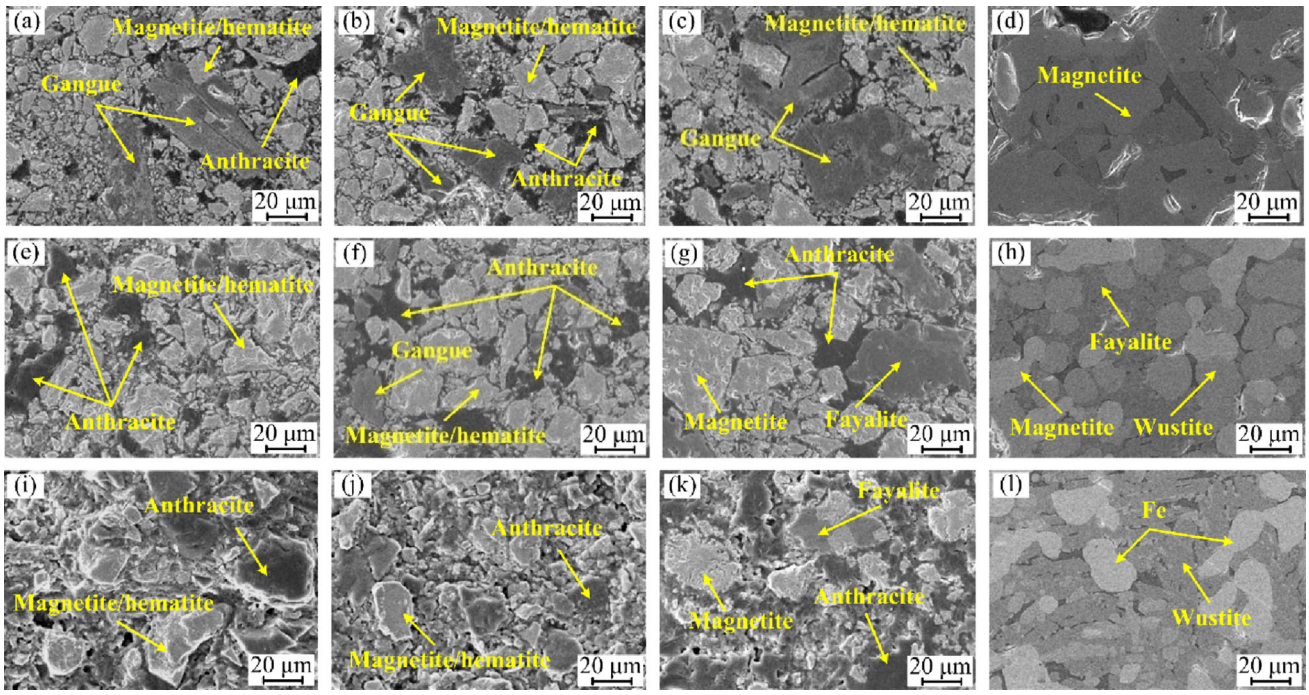

Fig. 9 Microstructure of reduced CIPWB with adding different ratios of anthracite under different temperatures. **a** 4% anthracite at 600 °C; **b** 4% anthracite at 800 °C; **c** 4% anthracite at 1000 °C; **d** 4% anthracite at 1150 °C; **e** 8% anthracite at 600 °C; **f** 8% anthracite at 800 °C; **g** 8% anthracite at 1000 °C; **h** 8% anthracite at 1150 °C; **i** 18% anthracite at 600 °C; **j** 18% anthracite at 800 °C; **k** 18% anthracite at 1000 °C; **l** 18% anthracite at 1150 °C

the consumption of anthracite inside the pellet are gradually intensified, leading to the remarkable increase in the porosity and shrinkage ratio. When the temperature is approximately 1000 °C, the porosity of pellet reaches the maximum value (46.82%). It should be noted that the thermal compressive strength of pellet is also relatively lower at this temperature, as seen in Fig. 7. As the temperature exceeds 1000 °C, further shrinkage of pellet is observed since a large amount of metallic iron is generated and connected, which contributes to the rapid decrease in the porosity of pellet and thereby improves the thermal compressive strength of pellet again.

According to the aforementioned analysis, when the reduction temperature is below 1000 °C, a small amount of reduction reaction occurs inside the CIPWB containing less than 8% anthracite due to the restricted availability of reducing agent. Consequently, Fe_3O_4 and Fe_2O_3 remain as the primary iron-bearing phases in the reduced pellet. In such circumstances, increasing the temperature is beneficial to the fragmentation of iron ore particles and to improving the meshing degree between the particles. As a result, an enhancement in thermal compressive strength of pellets is observed (as seen in Fig. 7). As the temperature is greater than 1000 °C, a large amount of reduction for iron oxides inside the pellet happens, and the reaction rate is accelerated, which contributes to the distinct decrease in the meshing degree between the particles since the porosity

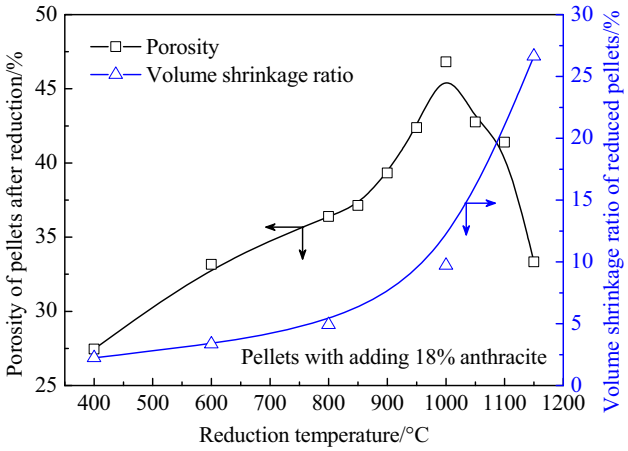

Fig. 10 Porosity and volume shrinkage of pellet with adding 18% anthracite during reduction process

of pellet increases. Eventually, the thermal strength is reduced. For the CIPWB with adding 18% anthracite (C/O = 1.0), when the reduction temperature is lower than 800 °C, the gasification reaction of carbon in anthracite is weak, resulting in a low level of pellet reduction rate. At this time, with increasing the temperature, the fragmentation of iron ore particles can still increase the meshing degree between the particles, which consequently contributes to a slight increase in the thermal strength of pellet. Moreover, as the temperature is 800–1000 °C, the

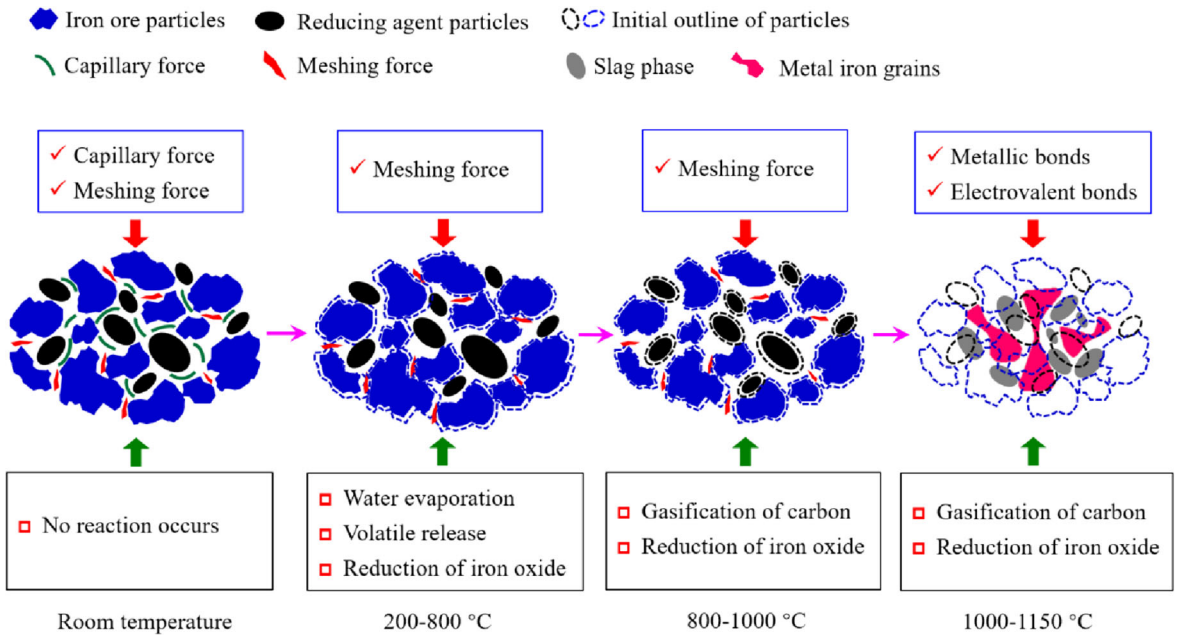

Fig. 11 Mechanism of thermal compressive strength evolution of CIPWB during reduction process

occurrence state of iron element in the pellet is transformed from Fe_3O_4 to FeO, and the reduction of iron oxides as well as the carbon gasification is gradually intensified, leading to the pellet becoming loose and thereby the decrease in thermal strength. When the reduction temperature exceeds 1000 °C, the iron-bearing phase primarily exists as connected metallic iron, which strengthens the internal structure of reduced pellet and leads to the gradual recovery of thermal strength.

In fact, the ratio of carbon in reducing agent to oxygen in iron oxides is generally not lower than 1.0 to ensure the metallization degree of carbon-bearing iron ore pellet during the actual production. Thus, the thermal strength of carbon-containing pellets during the reduction is affected by the evaporation of bound water, release of volatiles from reducing agent, gasification reaction of carbon, and reduction of iron oxide. The mechanism of thermal compressive strength evolution of CIPWB during the reduction process is demonstrated in Fig. 11. Notably, with the temperature rising, the variation in thermal compressive strength of CIPWB during the reduction process can be divided into three stages: (i) Thermal strength slowly increasing stage (specifically 200–800 °C). In this stage, the porosity of pellets increases due to the evaporation of water, the release of volatiles in reducing agent, and the preliminary reduction of iron oxide from Fe_2O_3 to Fe_3O_4, which can thus affect the pellet strength. However, with increasing the temperature, the fragmentation of iron ore particles in pellets enhances the meshing degree between the particles, which can improve the strength of pellet. As a result, the thermal strength of pellet slowly increases with the temperature rising. (ii) Thermal strength rapidly decreasing stage (800–1000 °C). In the stage, the gasification of carbon and the reduction of iron oxide are gradually intensified, and Fe_3O_4 is gradually reduced to FeO, which lead to the remarkable decrease in the particle size of reducing agent and the increase in the particle gap. As a result, the internal structure becomes porous, causing a substantial decrease in interparticle meshing degree and subsequently resulting in reduced pellet strength. (iii) Thermal strength recovering stage (1000–1150 °C). In this stage, the iron-bearing substance within the pellet is primarily in the form of metallic iron due to the vigorous reduction of iron oxide and carbon gasification. With increasing the temperature, the number of metallic iron grains rapidly increases, which are accumulated through extension, migration, and growth. Simultaneously, the gangue components undergo mineral reconstruction under the action of temperature. As a consequence, the thermal strength of pellet is gradually recovered.

4 Conclusions

1. During the low-temperature reduction process (300–500 °C), the thermal compressive strength of CIPWB linearly rises with increasing the pellet size under identical temperature and time. However, with increasing the anthracite ratio, the thermal compressive strength of CIPWB with similar size gradually decreases, and the decreased degree at 500 °C is significantly greater than that at 300 °C. When the

reduction temperature is 300 °C and the time is 30 min, the thermal compressive strength of the reduced pellet with adding 2% anthracite is enhanced from 9.73 to 31.03 N with the size of pellet increasing from 8.14 to 13.62 mm. As the temperature is 500 °C, with increasing the anthracite ratio from 2 to 8%, the thermal compressive strength of CIPWB with a reduction of 30 min decreases from 59.70 to 17.17 N.

2. During the high-temperature reduction process (600–1150 °C), the thermal compressive strength of CIPWB is markedly affected by the reduction temperature and the amount of anthracite. With increasing the temperature, the thermal compressive strength of pellet firstly increases and then decreases, while it gradually decreases with increasing the ratio of anthracite. Simultaneously, the temperature corresponding to the maximum thermal strength is gradually reduced with increasing the ratio of anthracite. For the CIPWB containing 8% anthracite, the thermal compressive strength of pellet is improved from 36.40 to 69.40 N as the temperature increases from 600 to 1020 °C and decreases to 19.50 N with further increasing the temperature to 1150 °C. When the anthracite ratio is 18%, the thermal strength of pellet reaches the maximum value (35.00 N) at 800 °C. Subsequently, it begins to decline, and the lowest value of thermal strength appears at 1050 °C, only 8.60 N. After that, the strength slowly increases.
3. The thermal compressive strength of carbon-bearing pellet is a macroscopic representation of the meshing mode and meshing degree between the particles inside pellet, which is related to several factors such as pellet size, reducing agent dosage, and reduction temperature. In the absence of binder, the evolution of thermal strength during the reduction process of CIPWB (C/O = 1.0) can be divided into three stages, namely thermal strength slowly increasing stage (200–800 °C), thermal strength rapidly decreasing stage (namely 800–1000 °C), and thermal strength recovering stage (1000–1150 °C).

Acknowledgements The authors gratefully acknowledge the financial support of the National Natural Science Foundation of China (52074080, 52004001, and 51574002).

Declarations

Conflict of interest Hong-ming Long is an editorial board member for *Journal of Iron and Steel Research International* and was not involved in the editorial review or the decision to publish this article. The author declares no conflict of interest.

References

[1] B.B. Lyu, G. Wang, F. Yang, H.B. Zuo, Q.G. Xue, J.S. Wang, J. Iron Steel Res. Int. 30 (2023) 2366–2377.
[2] T.D. Abhi, K. MacDermid-Watts, S.A. Salaudeen, A. Hayder, K.W. Ng, T. Todoschuk, A. Dutta, J. Sustain. Metall. 9 (2023) 927–949.
[3] H.T. Wang, M.S. Chu, J.W. Bao, Z.G. Liu, H.M. Long, J. Iron Steel Res. Int. 29 (2022) 741–750.
[4] M. Bailera, B. Rebolledo, Energ. Convers. Manage. 300 (2024) 117916.
[5] W. Zhang, J.M. Lei, J.Q. Li, G.J. Ma, H. Saxén, J. Iron Steel Res. Int. (2024) https://doi.org/10.1007/s42243-023-01141-x.
[6] H.J. Guo, J. Iron Steel Res. Int. 31 (2024) 46–63.
[7] G. Wang, J. Xu, K. He, Z.P. Zou, H. Bai, J. Iron Steel Res. Int. 31 (2024) 584–594.
[8] B. Rahmatmand, A. Tahmasebi, H. Lomas, T. Honeyands, P. Koshy, K. Hockings, A. Jayasekara, Fuel 336 (2023) 127077.
[9] R. Liu, Z.Y. Gao, H.Y. Li, X.J. Liu, Q. Lü, S.J. Chen, China Metallurgy (2024) https://doi.org/10.13228/j.boyuan.issn1006-9356.20230656.
[10] K. Nakano, H. Sakai, Y. Ujisawa, K. Kakiuchi, K. Nishioka, K. Sunahara, Y. Matsukura, H. Yokoyama, ISIJ Int. 62 (2022) 2424–2432.
[11] Y.B. Chen, Y.H. Yu, Y. Gao, J.S. Wang, Q.G. Xue, H.B. Zuo, J. Sustain. Metall. 9 (2023) 280–293.
[12] K.H. Ma, J.Y. Deng, G. Wang, Q. Zhou, J. Xu, Int. J. Hydrogen Energy 46 (2021) 26646–26664.
[13] L. Guo, Q.P. Bao, J.T. Gao, Q.S. Zhu, Z.C. Guo, ISIJ Int. 60 (2020) 1–17.
[14] J.L. Zhang, Z.J. Liu, K.X. Jiao, R.S. Xu, K.J. Li, Z.Y. Wang, C. Wang, Y.Z. Wang, L. Zhang, Chinese Journal of Engineering 43 (2021) 1630–1646.
[15] M.M. Sun, K.L. Pang, Z. Jiang, X.Y. Meng, Z.Y. Gu, J. Sustain. Metall. 9 (2023) 1399–1416.
[16] K. Iwase, T. Higuchi, T. Yamamoto, ISIJ Int. 63 (2023) 466–473.
[17] H.Y. He, H.L. Liu, Y.F. Cui, Y. Li, J. Ding, J. Iron Steel Res. 33 (2021) 196–201.
[18] S.F. Zhou, H.Y. Zheng, Y. Dong, X. Jiang, Q.J. Gao, F.M. Shen, Iron and Steel 56 (2021) No. 6, 15–20+27.
[19] R. Higashi, K. Owaki, D. Maruoka, T. Murakami, E. Kasai, ISIJ Int. 61 (2021) 1808–1813.
[20] H.H. Chang, I.G. Chen, K.M. Lu, S.H. Liu, ISIJ Int. 61 (2021) 2715–2723.
[21] B.F. Gandra, G.E. de Paula Junior, M.C. Bagatini, E. Osório, J. Mater. Res. Technol. 26 (2023) 6433–6445.
[22] R. Higashi, D. Maruoka, E. Kasai, T. Murakami, ISIJ Int. 63 (2023) 1972–1978.
[23] T. Murakami, R. Higashi, D. Maruoka, E. Kasai, ISIJ Int. 61 (2021) 2971–2978.
[24] J.H. Dong, G. Wang, H. Zhang, J.S. Wang, Q.G. Xue, China Metallurgy 31 (2021) No. 2, 90–94+108.
[25] T. Murakami, H. Shinomiya, D. Maruoka, E. Kasai, ISIJ Int. 59 (2019) 1011–1017.
[26] R.F. Wei, J.X. Li, G.W. Tang, D.Q. Cang, Ironmak. Steelmak. 41 (2014) 514–520.
[27] Y. Mochizuki, N. Tsubouchi, Metall. Mater. Trans. B 50 (2019) 2259–2272.
[28] A. Ayyandurai, J. Pal, Miner. Process. Extr. Metall. Rev. 43 (2022) 633–647.
[29] P. Yuan, B.X. Shen, D.P. Duan, G. Adwek, X. Mei, F.J. Lu, Energy 141 (2017) 472–482.
[30] T. Yang, J. Lei, X.J. Ren, Q.L. Wan, R.B. Zhou, H.M. Long, Iron and Steel 58 (2023) No. 4, 157–166.

[31] T. Yang, S. Liu, L.X. Qian, Z.M. Liu, Y.D. Pei, H.M. Long, J. Iron Steel Res. 34 (2022) 1047–1056.
[32] H.P. Lu, C.X. Yuan, G.Y. Sun, Sinter. Pelletiz. 48 (2023) No. 5, 79–85.
[33] X.J. Zhang, X.Y. Ding, J.S. Liu, T.H. Ju, J. Mater. Metall. 20 (2021) 57–63.
[34] S.L. Wu, F. Chang, J.L. Zhang, H. Lu, M.Y. Kou, ISIJ Int. 57 (2017) 1364–1373.
[35] S. Zhang, W. Ren, J.L. Li, X.F. Zhang, Metall. Res. Technol. 114 (2017) 101.
[36] S.Y. Xia, C.B. Hu, S.M. Zhang, R. Xue, Y.H. Xu, Journal of Solid Rocket Technology 35 (2012) 271–275.
[37] Q.M. Meng, R.F. Wei, J.X. Li, P. Wang, Z.F. Gao, Z.X. Di, H.M. Long, ISIJ Int. 58 (2018) 439–445.
[38] Q.M. Meng, Research on mechanical properties of carbon-bearing pellets and modification of its thermal strength, Anhui University of Technology, Ma'anshan, China, 2019.